PLOS ONE

RESEARCH ARTICLE

Mathematical modeling of the hematocrit influence on cerebral blood flow in preterm infants

Irina Sidorenko[1], Varvara Turova[2], Esther Rieger-Fackeldey[3], Ursula Felderhoff-Müser[4], Andrey Kovtanyuk[2], Silke Brodkorb[5], Renée Lampe[2]*

1 Chair of Mathematical Modeling, Mathematical Faculty, Technical University of Munich, Garching, Germany, **2** Research Unit for Pediatric Neuroorthopedics and Cerebral Palsy of the Buhl-Strohmaier Foundation, Orthopedic Department, School of Medicine, Klinikum rechts der Isar, Technical University of Munich, Munich, Germany, **3** Department of Pediatrics, School of Medicine, Klinikum rechts der Isar, Technical University of Munich, Munich, Germany, **4** Neonatology, Pediatric Intensive Care, Pediatric Neurology, Department of Pediatrics I, University Hospital Essen, University Duisburg-Essen, Essen, Germany, **5** Neonatology Department, Munich Clinic Harlaching, Munich, Germany

* renee.lampe@tum.de

Citation: Sidorenko I, Turova V, Rieger-Fackeldey E, Felderhoff-Müser U, Kovtanyuk A, Brodkorb S, et al. (2021) Mathematical modeling of the hematocrit influence on cerebral blood flow in preterm infants. PLoS ONE 16(12): e0261819. https://doi.org/10.1371/journal.pone.0261819

Editor: Adélia Sequeira, Universidade de Lisboa Instituto Superior Tecnico, PORTUGAL

Received: March 26, 2021

Accepted: December 10, 2021

Published: December 28, 2021

Data Availability Statement: Data are available from the media and publications repository of the Technical University of Munich (mediaTUM) at the following link: https://mediatum.ub.tum.de/1521746.

Funding: The authors I. Sidorenko and A. Kovtanyuk receive funding from Klaus Tschira Foundation (Grant number 00.302.2016). The author V. Turova receive funding from Buhl-Strohmaier Foundation. The author R. Lampe receive funding from Markus Würth Foundation.

Abstract

Premature birth is one of the most important factors increasing the risk for brain damage in newborns. Development of an intraventricular hemorrhage in the immature brain is often triggered by fluctuations of cerebral blood flow (*CBF*). Therefore, monitoring of *CBF* becomes an important task in clinical care of preterm infants. Mathematical modeling of *CBF* can be a complementary tool in addition to diagnostic tools in clinical practice and research. The purpose of the present study is an enhancement of the previously developed mathematical model for *CBF* by a detailed description of apparent blood viscosity and vessel resistance, accounting for inhomogeneous hematocrit distribution in multiscale blood vessel architectures. The enhanced model is applied to our medical database retrospectively collected from the 254 preterm infants with a gestational age of 23–30 weeks. It is shown that by including clinically measured hematocrit in the mathematical model, apparent blood viscosity, vessel resistance, and hence the *CBF* are strongly affected. Thus, a statistically significant decrease in hematocrit values observed in the group of preterm infants with intraventricular hemorrhage resulted in a statistically significant increase in calculated *CBF* values.

Introduction

Due to current knowledge and advances in neonatal care, 90% of preterm infants survive, but up to 50% of very low birth weight infants ($< 1500\ g$) develop some sort of permanent neurological impairment caused by injury to the preterm brain [1]. Intraventricular hemorrhage (*IVH*) remains the major complication of the premature birth, especially for very preterm infants with less than 32 weeks gestation (*WG*) [2]. At this age, a specific region containing a highly fragile vessel network, called germinal matrix (*GM*), is still present in the brain [3] and

The funders had no role in study design, data collection and analysis, decision to publish, or preparation of the manuscript.

Competing interests: The authors have declared that no competing interests exist.

can trigger development of *IVH*. Impaired cerebral autoregulation (cerebral pressure-passivity) in combination with variations in mean arterial pressure (*MAP*) and arterial carbon dioxide partial pressure (pCO_2) causes strong disturbances in cerebral blood flow (*CBF*) leading to *IVH* [4]. Therefore, implementation of regular monitoring of *CBF* in clinical routine is an important task for the care of preterm infants. Although several diagnostic techniques, such as near-infrared spectroscopy (*NIRS*) [5], Xenon-133 clearance measurements [6], transcranial Doppler ultrasonography [7], *MRI* based arterial spin labeling (*MRI ASL*) [8], and diffusion correlation spectroscopy (*DCS*) [5], have been developed during last few years, they are still not part of clinical routine monitoring. Therefore, mathematical assessment of the *CBF* can become a promising tool for *CBF* control in preterm infants in order to identify infants at risk.

A recently developed hierarchical cerebrovascular mathematical model [9–11] calculates *CBF* in the immature brain from clinically measured *MAP* and pCO_2 using a constant value of apparent blood viscosity. However, the vessel diameter and presence of blood cells suspended in blood plasma, especially red blood cells (*RBCs*), strongly influence the apparent viscosity of blood [12], and hence the resistance of the vessel network and *CBF*. The size of *RBCs* strongly affects the flow properties of blood in tubes with diameter less than 330 μm [12]. If *RBC*s are uniformly distributed throughout the vessel volume, their concentration can be measured as the systemic hematocrit (H_{SYS}). In the capillaries, *RBCs* collect near the centerline of the vessel, which leads to the formation of a cell free plasma layer adjacent to the vessel wall and, as a result, to a decreased concentration of *RBCs* known as Fåhraeus effect [13]. This reduced *RBCs* concentration can be described by the tube hematocrit (H_T), which is the volume fraction of *RBCs* that are inside the vessel at a given time instant. The net outcome of reduced *RBCs* concentration is a lower apparent viscosity in small arterioles (less than 200 μm in diameter) and capillaries, relative to the measured value in large feed arteries [14], which implies the reduction of flow resistance known as Fåhraeus-Lindqvist effect [15]. With decreasing capillary diameter, the apparent blood viscosity exhibits a further strong decrease reaching a minimum at about 6 μm [12]. For capillaries with diameters less than 6 μm the deformation of the erythrocytes takes place [16] and microvessel resistance can be described by an analytic formula [17] for the hydraulic resistance of capillary.

The purpose of the present work is the enhancement of the mathematical model for *CBF* calculation by a realistic description of apparent blood viscosity with accounting for inhomogeneous hematocrit distribution and its dependence on vessel diameter. For arteries and veins, a phenomenological dependence of the apparent viscosity on the vessel diameter [18, 19] is applied, whereas for capillaries a two-phase fluid model for single-file *RBCs* flow accounting for the deformation of *RBCs* in thin vessels [16, 17, 20] is employed. The performance of the enhanced model is demonstrated using clinical data recorded during regular monitoring of 254 preterm infants with the gestational age of 23–30 weeks. The effect of hematocrit value on vessel resistance and *CBF* as well as on differentiation between preterm infants with and without *IVH* is shown.

Materials and methods

Clinical data

Clinical data were obtained from the records of 254 preterm infants treated in the Department of Neonatology at the University Hospital Essen and the Department of Pediatrics of the School of Medicine, Klinikum rechts der Isar, Technical University of Munich. The study was approved by the ethical committee of the University Hospital Essen, University Duisburg-Essen (Ref. 16-7284-BO) and ethical committee of the School of Medicine, Klinikum rechts der Isar, Technical University of Munich (Ref. 364/15). No informed consent from parents

Table 1. Basic demographic characteristics of the study cohort.

Parameter	All n = 254 (100%)	No *IVH* n = 118 (100%)	With *IVH* n = 136 (100%)	*p*-value*
Gestational age [*WG*]	26.46 ± 2.11	26.68 ±2.17	26.26 ± 2.04	0.13
Birth weight [*g*]	864.06 ± 279.10	850.68 ± 252.81	875.66 ± 300.50	0.70
Male	122 (48.03%)	48 (40.68%)	74 (54.4%)	0.03
Twins	64 (25.19%)	27 (22.88%)	37 (27.21%)	0.55
Triplets	31 (12.21%)	16 (13.56%)	15 (11.03%)	0.69
In Vitro Fertilization	32 (12.6%)	17 (14.4%)	15 (11.0%)	0.51
Natural birth	22 (8.66%)	7 (5.93%)	15 (11.03%)	0.18

*p-value is given for difference between control (no *IVH*) and affected (with *IVH*) groups.

https://doi.org/10.1371/journal.pone.0261819.t001

was necessary because it was a retrospective study. The clinical records have been collected over 11 years (between 01.2006 and 12.2016) and were fully anonymized before data transfer from the neonatal units to the research group. The gestational age of the sample group ranged from 23 to 30 weeks gestation (*WG*) and a body weight from 335 *g* to 1580 *g*. Preterm infants without *IVH* (118) served as control group and those with *IVH* (136) as affected group. Basic demographic characteristics of the cohort are presented in Table 1, in which continuous variables are expressed as mean and standard deviation, while categorical variables are presented as the number of cases and percentages. *IVH* was diagnosed by serial cranial ultrasound examinations and *IVH* severity was classified according to the Papile grading system [21]. *MAP*, pCO_2 and H_{SYS} were collected as standard routine clinical data during the first 10 days after birth in the control group, and for up to 7 consecutive days before and 3 days after hemorrhage in the affected group. All pCO_2 values were taken from the capillary or arterial blood gas analysis. Corresponding *MAP* measurements were taken at the same time as blood gas analysis and corresponding H_{SYS} values were taken from the last available laboratory record. Since intracranial pressure P_{ic} could not be recorded in preterm infants, a constant $P_{ic} = 5\ mmHg$ [22] was used for numerical calculations for all infants. Statistical analysis of clinical parameters and calculated *CBF* was done using the two-sided Wilcoxon's rank-sum test for continuous variables and Fisher's exact test for categorical parameters (MATLAB2020a) with a p-value less than 0.05 considered to be statistically significant.

Modeling of *CBF* in immature brain with germinal matrix

A mathematical model for the calculation of *CBF* [10, 11] in the immature brain was derived from a hierarchical cerebrovascular model for the adult brain [9]. In this model, the cerebral vascular system is divided into 19 levels connected in series according to morphological vessel characteristics. Additionally, each level consists of m_j parallel connected vessels. Thus, the total *CBF* is calculated from Kirchhoff's law as follows:

$$CBF = (MAP - P_{ic})/RES,$$

$$RES = \sum_{j=1}^{19} RES_j^{level}, RES_j^{level} = RES_j/m_j.$$

Here *RES* is the total cerebrovascular resistance, RES_j^{level} is the resistance of vascular level j, and RES_j is the resistance of single vessel on level j ($j = 1...19$).

On each level, the number of vessels m_j as well as their lengths l_j and diameters d_j are scaled according to the brain weight of each infant estimated from their birth weight [23].

Furthermore, a vascular response on changes of MAP and pCO_2 is incorporated into the model through an increase or decrease of vessel diameter (i.e., vasodilation or vasoconstriction).

The presence of germinal matrix is modeled as an additional parallel circuit in the capillary level ($j = 10$). Thus, the total resistance of capillary level RES_{10}^{level} is calculated from the resistance of the GM capillaries RES_{10}^{GM} and the resistance of the rest, non-GM brain capillaries RES_{10}^{nGM} as:

$$RES_{10}^{level} = \left(\left(RES_{10}^{GM} \right)^{-1} + \left(RES_{10}^{nGM} \right)^{-1} \right)^{-1},$$

$$RES_{10}^{GM,nGM} = RES_{GM,nGM} / m_{GM,nGM}$$

Here RES_{GM} and RES_{nGM} are the resistances of the individual GM and non-GM capillaries. The corresponding number of vessels m_{GM} and m_{nGM} are estimated according to the gestational age and brain weight of each infant.

A resistance of individual vessel RES_j is calculated by the application of a micropolar fluid model [24, 25] accounting for the presence of rigid, randomly oriented particles ($RBCs$) suspended in a viscous medium. Simplified analytic expressions for the flow velocity profile and hydraulic resistance are derived using power series expansions, based on the description [26, 27] of steady-state flow of micropolar fluid through a pipe with circular cross-section. In this method, a constant value $\mu = 0.003\ pa \cdot s$ of apparent blood viscosity is used. Knowing the resistance of individual vessel and global CBF, one can calculate blood flow in individual vessel on level j as follows:

$$CBF_j = CBF \cdot RES_j^{level} / RES_j.$$

Accounting for the hematocrit in large vessels

To account for the influence of hematocrit on the resistance of large vessels, the constant blood viscosity is replaced by the apparent blood viscosity μ_a, which depends on the vessel diameter and concentration of RBCs (hematocrit).

For arteries and veins with diameter $d > 500\ \mu m$ apparent blood viscosity is an almost constant value, which depends only on hematocrit [28]. However, with decreasing vessel diameter the Fåhraeus-Lindqvist effect [15] takes place, resulting in lower viscosity compared to larger vessels. In order to take this effect into account, the calculation of RES_j is done using "*in vivo* viscosity law" developed in [18] and widely applied in numerical simulations [19, 29, 30]. In this phenomenological relationship, variations of apparent viscosity of blood are described as a function of diameter $d\ \mu m$ by the following set of formulas:

$$\mu_a = \mu_{PL} \left[1 + (\mu_{0.45} - 1) \cdot \frac{(1 - H_D)^C - 1}{(1 - 0.45)^C - 1} \cdot \left(\frac{d}{d - 1.1} \right)^2 \right] \cdot \left(\frac{d}{d - 1.1} \right)^2,$$

$$\mu_{0.45} = 6 \cdot exp(-0.085 \cdot d) + 3.2 - 2.44 \cdot exp(-0.06 \cdot d^{0.645}),$$

$$C = \left(0.8 + e^{-0.075 \cdot d} \right) \cdot \left(-1 + \frac{1}{1 + 10^{-11} \cdot d^{12}} \right) + \frac{1}{1 + 10^{-11} \cdot d^{12}}.$$

Here $\mu_{PL} = 0.001\ Pa \cdot s$ is the viscosity of plasma [17, 30] and H_D is the discharge hematocrit which is defined by the ratio between red blood cell volume and total blood volume. Experimental measurements have shown [31] that the discharge hematocrit H_D is similar to the

systemic hematocrit H_{SYS} taken from arterioles or venules with diameter 6.98 μm. Therefore, in numerical calculations we take discharge hematocrit H_D equal to the clinically measured systemic hematocrit H_{SYS}.

Accounting for the tube hematocrit in capillaries

In capillaries with diameter $d_j < 10\ \mu m$ ($j = 10$) the blood plasma moves in a cell-free layer near the wall, whereas *RBC*s travel through the vessel in somewhat of a single file line [13, 17]. The resistance of individual *GM* or non-*GM* capillary $RES_{GM,nGM}$ is calculated by the application of two-phase fluid model with single-file *RBC* flow [17, 20] as:

$$RES_{GM,nGM} = \rho + (\hat{\rho} - \rho)H_T$$

Here, H_T is a tube hematocrit and ρ and $\hat{\rho}$ are defined [17] as:

$$\hat{\rho} = \frac{8l}{\pi} \cdot \left(\frac{r_{GM,nGM}^4 - r_0^4}{\mu_{PL}} + \frac{r_0^4}{\mu_{RBC}} \right)^{-1},$$

$$\rho = \frac{8l}{\pi} \left(\frac{r_{GM,nGM}^4}{\mu_{PL}} \right)^{-1},$$

$$r_0 = 0.3\mu m + 0.8 \cdot r_{GM,nGM},$$

$$\mu_{PL}(H_T) = 0.001 \cdot (16 + 5H_T)/15\ \ Pa \cdot s,$$

$$\mu_{RBC} = 0.1\ \ Pa \cdot s.$$

The reduction of the tube hematocrit H_T in vessels with diameter $d\ \mu m$ is estimated from the discharge hematocrit H_D as [32]:

$$H_T/H_D = H_D + (1 - H_D) \cdot \left(1 + 1.7 \cdot e^{-0.35 \cdot d} - 0.6 \cdot e^{-0.01 \cdot d}\right).$$

As in the previous section, the discharge hematocrit H_D equals to the clinically measured systemic hematocrit H_{SYS}.

Results

The variation of apparent blood viscosity depending on vessel diameter is shown in Fig 1a for several values of systemic hematocrit H_{SYS}. For vessels with $d > 500\ \mu m$ the apparent blood viscosity is almost independent on vessel diameter (Fig 1a) and for $H_{SYS} = 45\%$ it is close to the constant value $\mu = 0.003\ Pa \cdot s$, which is usually taken for numerical calculations. However, the rise or reduction of systemic hematocrit causes a corresponding increase or decrease of the apparent viscosity (see Table 2). For vessels with $d < 30\ \mu m$ a strong nonlinear increase of apparent viscosity can be caused both by the increase of hematocrit and decrease of diameter. Thus, for vessels with $d = 10\ \mu m$ and $H_{SYS} = 60\%$ the apparent viscosity can be more than three times higher than the constant value $\mu = 0.003\ Pa \cdot s$ (see Table 2).

The values of the apparent viscosity with accounting of H_{SYS} and individual vessel diameter d_j (Fig 1a) are used for the calculation of the individual vessel resistance RES_j on each level j of the hierarchical cerebrovascular model (Fig 2a). The resistance of individual vessels rises with an increase in hematocrit and a decrease in diameter. The resistances of *GM* and non-*GM* capillaries are computed with the two-phase fluid model using tube hematocrit H_T. The latter

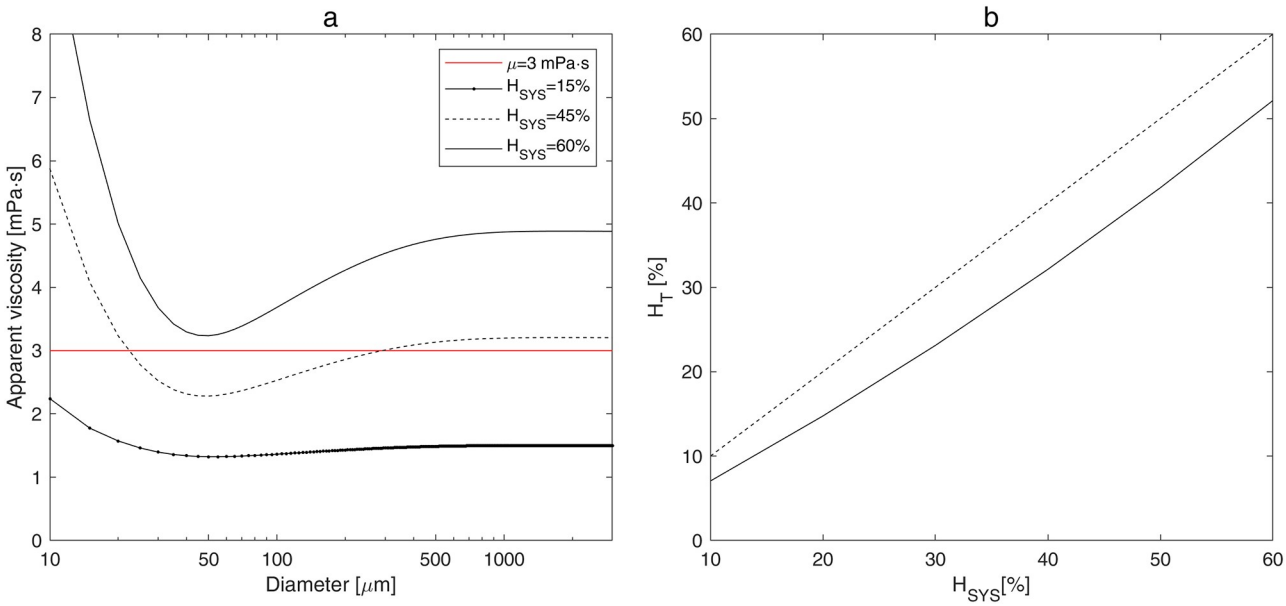

Fig 1. Calculated apparent blood viscosity and tube hematocrit. (a) Calculated apparent blood viscosity versus diameter of vessel for different values of systemic hematocrit. (b) Tube hematocrit versus systemic hematocrit (dashed line $H_T = H_{SYS}$ is shown for comparison).

https://doi.org/10.1371/journal.pone.0261819.g001

is calculated with accounting for Fåhraeus effect resulting in the reduction of the H_T value with respect to the H_{SYS} value, which is shown in Fig 1b. The resistance of a single *GM* capillary is lower than that of a non-*GM* capillary (Table 2) because of the difference in diameters (*GM* capillaries have larger diameter than non-*GM* ones).

The total resistance of the whole vascular level RES_j^{level} in the hierarchical cerebrovascular model depends on the resistance of a single vessel RES_j and the number of the vessels on every level *j*. The resistances RES_j^{level} calculated for 25 *WG* are shown in Fig 2b. The largest resistance is obtained for the precapillary layer ($j = 9$) with the smallest arterioles. On the capillary level,

Table 2. Dependence of computed model parameters on hematocrit.

Hematocrit [%]	H_{SYS}		15	45	60
	H_T		10.8	36.9	52.1
Apparent blood viscosity $[10^{-3}\ Pa \cdot s]$	μ	$d = 10\mu m$	2.24	5.87	9.83
		$d = 500\mu m$	1.49	3.1	4.76
Resistance of individual vessel $[10^{16}\ Pa \cdot s/m^3]$ ***WG* = 25**	RES_9		0.789	1.95	3.03
	RES_{GM}		1.03	1.51	1.82
	RES_{nGM}		3.34	5.16	6.33
Resistance of vascular level $[10^8\ Pa \cdot s/m^3]$ ***WG* = 25**	RES_9^{level}		22.2	54.2	85.1
	RES_{10}^{level}		14.8	22.7	27.8
	RES_{10}^{GM}		164	239	288
	RES_{10}^{nGM}		16.2	25.1	30.8
Total resistance $[10^8\ Pa \cdot s/m^3]$	*RES*	*WG* = 25	74.6	142	209
		WG = 30	34.7	65.9	96.9
Cerebral blood flow $[ml/min/100\ g]$	*CBF*	*WG* = 25	16.5	8.64	5.87
		WG = 30	19.9	10.5	7.11

https://doi.org/10.1371/journal.pone.0261819.t002

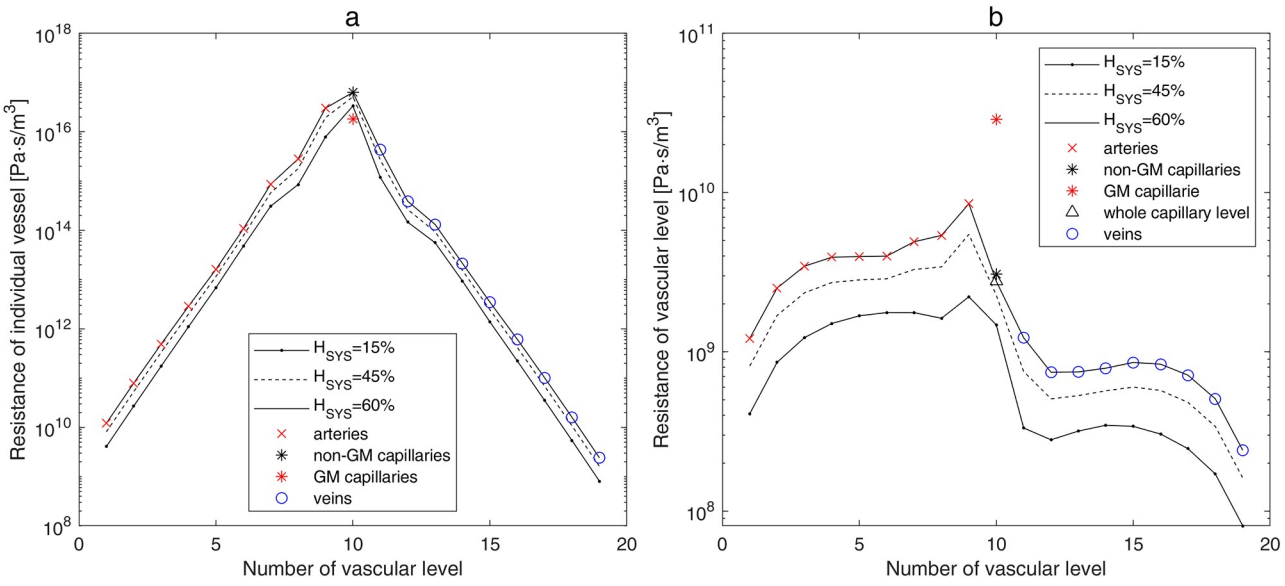

Fig 2. Calculated resistance of the individual vessel (a) and of the whole vascular level (b) for different values of systemic hematocrit.

https://doi.org/10.1371/journal.pone.0261819.g002

there is considerable difference in two parallel connected regions (*GM* and non-*GM*) regarding the number of vessels and, consequently, different resistances. Namely, the *GM* has a lower number of vessels and a higher resistance than the rest (non-*GM)* brain region. In our example of a preterm infant with 25 *WG* (Table 2), the increase in hematocrit from H_{SYS} = 15% (H_T = 10.8%) to H_{SYS} = 45% (H_T = 36.9%) results in the increase of the RES_{10}^{GM} from $163.9 \cdot 10^8$ to $238.6 \cdot 10^8 Pa \cdot s/m^3$ and of the RES_{10}^{nGM} from $16.2 \cdot 10^8$ to $25.1 \cdot 10^8 Pa \cdot s/m^3$, which is in good agreement with values presented by [17]. For higher values of H_{SYS} the total resistance of the vascular levels continues to rise (Fig 2b).

The effect of hematocrit on the total cerebrovascular resistance *RES* and *CBF* is shown for gestational ages ranging from 23 to 36 *WG* in Fig 3 and for *WG* = 25 and *WG* = 30 in Table 2. Both the reduction of hematocrit and increase of gestational age cause a decrease of the total vascular resistance, resulting in an increase of *CBF*. For all gestational ages, the reduction of H_{SYS} from 60% to 45% results in 1.5-fold increase of *CBF*; further reduction of H_{SYS} from 45% to 15% results in 1.9-fold increase of *CBF*.

The model developed was applied to clinical records of 254 preterm infants with gestational age ranged from 23 to 30 *WG*. Statistical analysis revealed that the demographic factors did not affect the hematocrit (Table 3). Moreover, the mean hematocrit in the control group (Table 3, no *IVH*) was close to the value of 45% usually taken for numerical calculations (Fig 4a). Therefore, no significant changes (Table 4) in the calculated *CBF* for the control group were obtained due to including measured hematocrit in the mathematical model (Fig 4b). However, the mean value of the hematocrit in the affected group was significantly lower than that in the control group (Table 3). As a result, *CBF* calculated using the measured hematocrit was higher in the affected group (Fig 4b) and this increase was significant for *IVH* grades III+IV (Table 4). This effect was even more noticeable for capillary vessels (Table 5): the increase of *CBF* in individual capillary was statistically significant not only for severe *IVH* (grades III-IV), but already for moderate *IVH* (grad II).

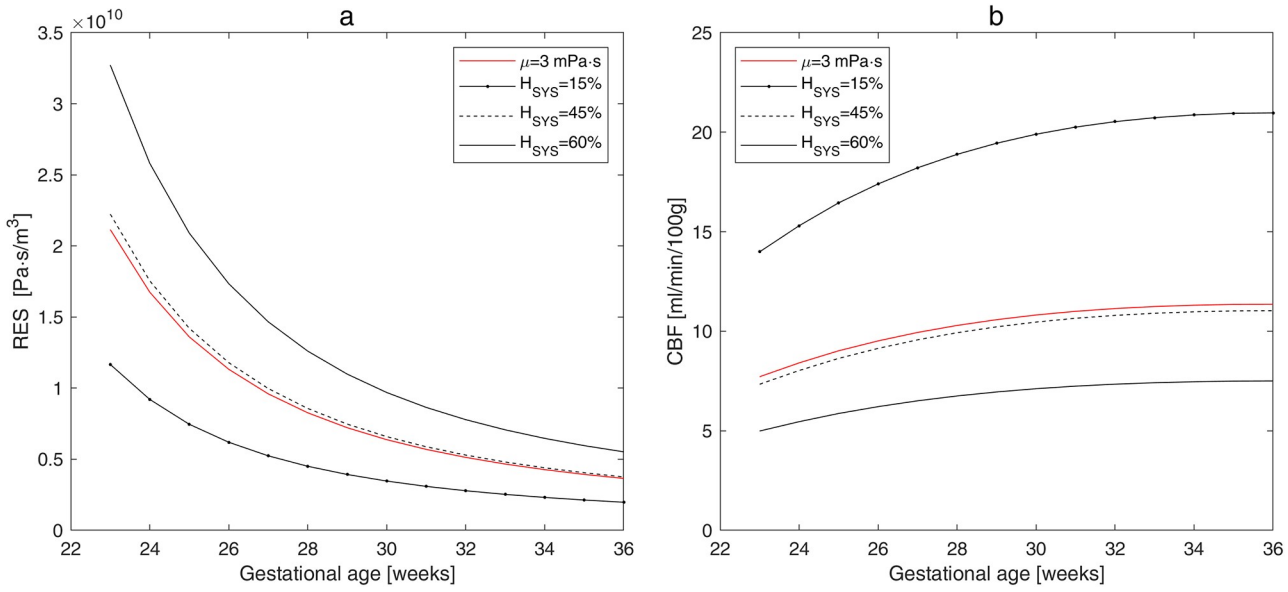

Fig 3. Calculated total cerebral resistance (a) and *CBF* (b) versus gestational age for different values of systemic hematocrit. The red lines show the values calculated using the constant blood viscosity $\mu = 0.003\ Pa \cdot s$.

https://doi.org/10.1371/journal.pone.0261819.g003

Table 3. Dependence of the hematocrit on basic demographic characteristics and *IVH* diagnosis.

Parameter	no	yes	*p*-value
Male	42.80 ± 7.49	42.70 ± 8.22	0.72
Multiple birth	42.68 ± 7.59	42.93 ± 8.39	0.72
In Vitro Fertilization	42.85 ± 7.90	41.78 ± 7.14	0.95
Natural birth	42.75 ± 7.98	42.82 ± 6.82	0.65
IVH	45.14 ± 7.92	41.41 ± 7.48	0.01

https://doi.org/10.1371/journal.pone.0261819.t003

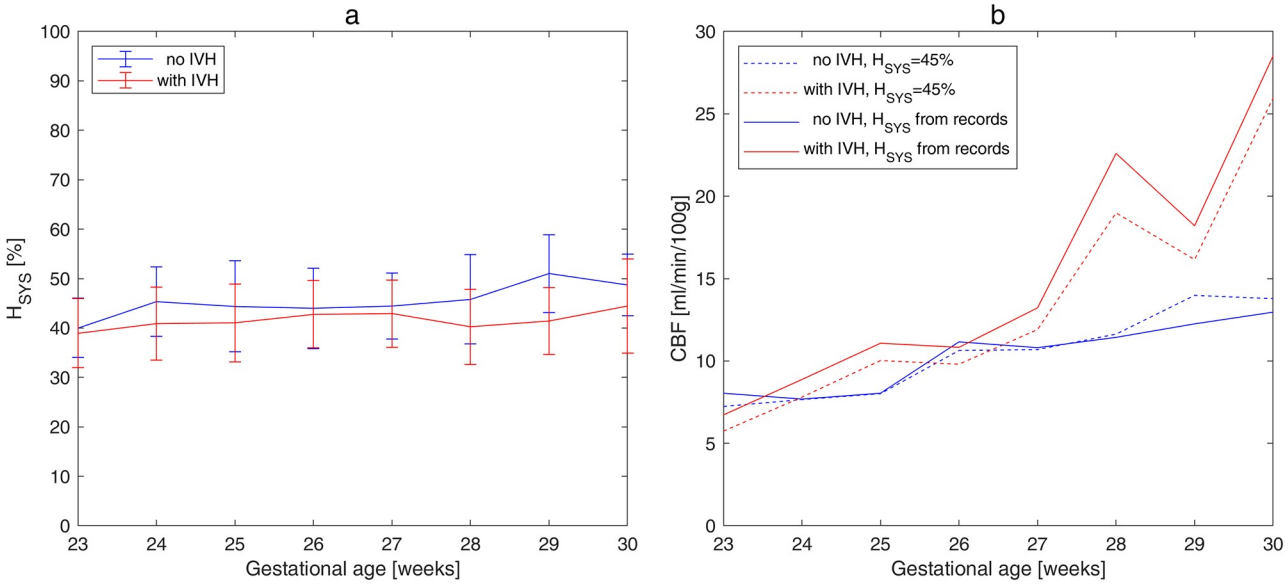

Fig 4. Mean values with standard deviations averaged over gestational age. (a) Measured systemic hematocrit. (b) *CBF* calculated for $H_{SYS} = 45\%$ (dashed lines) and for H_{SYS} from clinical records (solid lines).

https://doi.org/10.1371/journal.pone.0261819.g004

Table 4. Global *CBF* [*ml/min*/100 *g*] for different values of H_{SYS}.

IVH	H_{SYS} = 45%	H_{SYS} from records	*p*-value
No (n = 118)	9.48 ± 4.57	9.53 ± 4.95	0.79
All Grades (n = 136)	11.39 ± 9.24	12.92 ± 11.31	0.004
Grade I (n = 38)	12.28 ± 6.28	13.24 ± 7.7	0.53
Grade II (n = 42)	10.87 ± 10.98	12.23 ± 12.62	0.09
Grade III+IV (n = 48+8)	11.45 ± 8.85	13.22 ± 11.37	0.016

https://doi.org/10.1371/journal.pone.0261819.t004

Table 5. *CBF* in individual capillary [10^{-6} *ml/min*/100 *g*] for different values of H_{SYS}.

IVH	H_{SYS} = 45%	H_{SYS} from records	*p*-value
No (n = 118)	1.48 ± 0.63	1.49 ± 0.69	0.77
All Grades (n = 136)	1.49 ± 0.80	1.68 ± 1.00	<0.001
Grade I (n = 38)	1.62 ± 0.75	1.78 ± 1.02	0.36
Grade II (n = 42)	1.48 ± 0.85	1.64 ± 0.98	0.007
Grade III+IV (n = 48+8)	1.46 ± 0.78	1.66 ± 1.01	0.002

https://doi.org/10.1371/journal.pone.0261819.t005

Discussion

Blood hematocrit is an important factor influencing apparent blood viscosity, vessel resistance and blood flow [33, 34]. In the present work, the previously developed hierarchical cerebrovascular model for *CBF* calculation [10, 11] was enhanced by including effects of inhomogeneous hematocrit and vessel diameter on the apparent blood viscosity, vessel resistance and hence *CBF*. The dependence of the apparent viscosity on blood hematocrit and vessel diameter was modeled according to the "*in vivo* viscosity law" derived from experimental data [18]. Calculated values of apparent viscosity were used for the computation of the individual vessel resistance on each level of the hierarchical cerebrovascular mode. Additionally, two-phase fluid model [17] was used for the calculation of the resistance of *GM* and non-*GM* capillaries.

In mathematical modeling performed in the present study, the reduction of hematocrit caused a decrease in the apparent blood viscosity and vascular resistance, resulting in an increase of *CBF*. Our numerical results are in good agreement with values from literature. The apparent blood viscosity calculated for different hematocrit values and vessel diameters were close to the experimental data presented by [12] and the observations by [35] showing twofold increase of the apparent viscosity with an increase of hematocrit from 40% to 60%. In our calculations for vessels with diameter 10 μm, a hematocrit increase from 45% to 60% resulted in 1.67-fold increase of the apparent viscosity (see Table 2).

The apparent viscosity of the individual vessel was used for the calculation of total cerebrovascular resistance that depends on the resistance of the individual vessel and number of vessels on each vascular level. In our model, the largest resistance was obtained for the precapillary layer with the smallest arterioles, which is consistent with the previous observations [4, 36, 37]. On capillary level, the concentration of *RBC*s near the center of the capillary [13] results in the reduction of hematocrit to a value known as tube hematocrit. We used tube hematocrit values estimated from the systemic hematocrit [32] for the calculation of vascular resistances for two brain regions, namely, the *GM* and the rest, non-*GM*, part of the brain [17]. The *GM* and non-*GM* resistances calculated in our study for 25 *WG* (Table 2) showed the same dependence on hematocrit as in [17].

Mathematical modeling revealed an inverse relationship between *CBF* and hematocrit, which is consistent with experimental studies [37, 38]. A regression analysis based on the

xenon-133 measurements of *CBF* in 15 preterm infants with mean gestational age 31 *WG* [38] has demonstrated a significant inverse correlation between *CBF* and hematocrit with the slope -2.3 for the hematocrit variation from 24% to 48%. These results are similar to the 1.9-fold *CBF* increase caused by the hematocrit decrease from 45% to 15% demonstrated for *WG* = 30 in the present study.

The enhanced mathematical model was applied to clinical data collected retrospectively from medical records of 254 preterm infants with gestational age 23–30 weeks. Including the clinically measured hematocrit in the model led to an increase of calculated *CBF* in preterm infants with *IVH* diagnosis. The increase was statistically significant for severe *IVH* (grade III+IV). These results are in agreement with observations that a relatively low hematocrit during the first 24 hours of life correlates with a high incidence of *IVH* [39, 40] and is associated with a prolonged bleeding time [41]. Another important result was the increase of *CBF* in capillary vessels, which was statistically significant for preterms with moderate (grad II) and severe (grad III+IV) *IVH*. Increased *CBF* values in capillary vessels may explain experimental observations that hemorrhage in immature brain often originates from capillary bed or in capillary-vein junction [42]. The exact location of vessel rupture is still under discussion [43] and cannot be determined by the mathematical model used in this study. Thus, the mathematical model developed has demonstrated a correct relationship between decreased hematocrit and enhanced risk of *IVH* in preterm infants.

The following limitations need to be addressed. Whereas some experimental observations demonstrate that *RBCs* aggregation into clusters [35] contribute to the viscosity reduction, these effects were not simulated in the present study. In addition, the influence of the plasma viscosity was not investigated, although some data suggest that plasma viscosity may be more important in the regulation of *CBF* than whole blood viscosity [33]. The effects of *RBCs* aggregation and increased plasma viscosity on *CBF* are considered for further development of the mathematical model for *CBF* calculation.

Conclusions

The mathematical model for *CBF* calculation has been developed further, by accounting for the effect of inhomogeneous hematocrit on the apparent blood viscosity and vessel resistance. The model is in good agreement with published experimental results. It has been shown that including the clinically measured hematocrit in the mathematical model strongly effects the apparent blood viscosity, vessel resistance and hence *CBF*. Furthermore, in the group of preterm infants with *IVH* diagnosis, the inclusion of measured hematocrit values resulted in a statistically significant increase of calculated *CBF* values compared to calculations with a constant hematocrit value. Thus, accounting for the effect of hematocrit on *CBF* may improve clinical monitoring of preterm infants and prediction of *IVH* development.

Acknowledgments

Renée Lampe appreciates the Markus Würth Professorship at the Technical University of Munich.

Author Contributions

Conceptualization: Renée Lampe.

Data curation: Irina Sidorenko, Esther Rieger-Fackeldey, Ursula Felderhoff-Müser, Silke Brodkorb.

Formal analysis: Irina Sidorenko, Varvara Turova, Andrey Kovtanyuk.

Funding acquisition: Renée Lampe.

Investigation: Varvara Turova, Andrey Kovtanyuk.

Methodology: Irina Sidorenko, Varvara Turova, Esther Rieger-Fackeldey, Ursula Felderhoff-Müser, Silke Brodkorb, Renée Lampe.

Project administration: Renée Lampe.

Resources: Renée Lampe.

Software: Irina Sidorenko.

Supervision: Ursula Felderhoff-Müser, Renée Lampe.

Validation: Irina Sidorenko, Varvara Turova, Andrey Kovtanyuk.

Visualization: Irina Sidorenko, Andrey Kovtanyuk.

Writing – original draft: Irina Sidorenko.

Writing – review & editing: Irina Sidorenko, Varvara Turova, Esther Rieger-Fackeldey, Ursula Felderhoff-Müser, Andrey Kovtanyuk, Silke Brodkorb, Renée Lampe.

References

1. Babcock MA, Kostova FV, Ferriero DM, Johnston MV, Brunstrom JE, Hagberg H, et al. Injury to the preterm brain and cerebral palsy: clinical aspects, molecular mechanisms, unanswered questions, and future research directions. Journal of child neurology. 2009 Sep; 24(9):1064–84. https://doi.org/10.1177/0883073809338957 PMID: 19745084
2. Blencowe H, Cousens S, Chou D, Oestergaard M, Say L, Moller AB, et al. Born too soon: the global epidemiology of 15 million preterm births. Reproductive health. 2013 Nov; 10(1):1–4. https://doi.org/10.1186/1742-4755-10-S1-S2 PMID: 24625129
3. Kinoshita Y, Okudera T, Tsuru E, Yokota A. Volumetric analysis of the germinal matrix and lateral ventricles performed using MR images of postmortem fetuses. American Journal of Neuroradiology. 2001 Feb 1; 22(2):382–8. PMID: 11156787
4. Ballabh P. Intraventricular hemorrhage in premature infants: mechanism of disease. Pediatric research. 2010 Jan; 67(1):1–8. https://doi.org/10.1203/PDR.0b013e3181c1b176 PMID: 19816235
5. Diop M, Kishimoto J, Toronov V, Lee DS, Lawrence KS. Development of a combined broadband near-infrared and diffusion correlation system for monitoring cerebral blood flow and oxidative metabolism in preterm infants. Biomedical optics express. 2015 Oct 1; 6(10):3907–18. https://doi.org/10.1364/BOE.6.003907 PMID: 26504641
6. Jayasinghe D, Gill AB, Levene MI. CBF reactivity in hypotensive and normotensive preterm infants. Pediatric research. 2003 Dec; 54(6):848–53. https://doi.org/10.1203/01.PDR.0000088071.30873.DA PMID: 12904589
7. Noori S, Anderson M, Soleymani S, Seri I. Effect of carbon dioxide on cerebral blood flow velocity in preterm infants during postnatal transition. Acta Paediatrica. 2014 Aug; 103(8):e334–9. https://doi.org/10.1111/apa.12646 PMID: 24673183
8. De Vis JB, Hendrikse J, Groenendaal F, De Vries LS, Kersbergen KJ, Benders MJ, et al. Impact of neonate haematocrit variability on the longitudinal relaxation time of blood: Implications for arterial spin labelling MRI. NeuroImage: Clinical. 2014 Jan 1; 4:517–25.
9. Piechnik SK, Chiarelli PA, Jezzard P. Modelling vascular reactivity to investigate the basis of the relationship between cerebral blood volume and flow under CO2 manipulation. Neuroimage. 2008 Jan 1; 39(1):107–18. https://doi.org/10.1016/j.neuroimage.2007.08.022 PMID: 17920935
10. Lampe R, Botkin N, Turova V, Blumenstein T, Alves-Pinto A. Mathematical modelling of cerebral blood circulation and cerebral autoregulation: towards preventing intracranial hemorrhages in preterm newborns. Computational and mathematical methods in medicine. 2014 Oct; 2014:965275. https://doi.org/10.1155/2014/965275 PMID: 25126111
11. Sidorenko I, Turova V, Botkin N, Eckardt L, Alves-Pinto A, Felderhoff-Müser U, et al. Modeling cerebral blood flow dependence on carbon dioxide and mean arterial blood pressure in the immature brain with

accounting for the germinal matrix. Frontiers in neurology. 2018 Oct 9; 9:812. https://doi.org/10.3389/fneur.2018.00812 PMID: 30356709

12. Pries AR, Secomb TW, Gaehtgens P. Biophysical aspects of blood flow in the microvasculature. Cardiovascular research. 1996 Oct 1; 32(4):654–67. PMID: 8915184
13. Fåhraeus R. The suspension stability of the blood. Physiological Reviews. 1929 Apr 1; 9(2):241–74.
14. Lipowsky HH, Usami S, Chien S, Pittman RN. Hematocrit determination in small bore tubes from optical density measurements under white light illumination. Microvascular research. 1980 Jul 1; 20(1):51–70. https://doi.org/10.1016/0026-2862(80)90019-9 PMID: 7412586
15. Fåhraeus R, Lindqvist T. The viscosity of the blood in narrow capillary tubes. American Journal of Physiology-Legacy Content. 1931 Mar 1; 96(3):562–8.
16. Secomb TW, Hsu R, Pries AR. Motion of red blood cells in a capillary with an endothelial surface layer: effect of flow velocity. American Journal of Physiology-Heart and Circulatory Physiology. 2001 Aug 1; 281(2):H629–36. https://doi.org/10.1152/ajpheart.2001.281.2.H629 PMID: 11454566
17. Botkin ND, Kovtanyuk AE, Turova VL, Sidorenko IN, Lampe R. Accounting for tube hematocrit in modeling of blood flow in cerebral capillary networks. Computational and mathematical methods in medicine. 2019 Aug 18;2019. https://doi.org/10.1155/2019/4235937 PMID: 31531122
18. Pries AR, Secomb TW, Gessner T, Sperandio MB, Gross JF, Gaehtgens P. Resistance to blood flow in microvessels in vivo. Circulation research. 1994 Nov; 75(5):904–15. https://doi.org/10.1161/01.res.75.5.904 PMID: 7923637
19. Lorthois S, Cassot F, Lauwers F. Simulation study of brain blood flow regulation by intra-cortical arterioles in an anatomically accurate large human vascular network. Part II: flow variations induced by global or localized modifications of arteriolar diameters. Neuroimage. 2011 Feb 14; 54(4):2840–53. https://doi.org/10.1016/j.neuroimage.2010.10.040 PMID: 21047557
20. Obrist D, Weber B, Buck A, Jenny P. Red blood cell distribution in simplified capillary networks. Philosophical Transactions of the Royal Society A: Mathematical, Physical and Engineering Sciences. 2010 Jun 28; 368(1921):2897–918. https://doi.org/10.1098/rsta.2010.0045 PMID: 20478913
21. Papile L-A, Burstein J, Burstein R, Koffler H. Incidence and evolution of subependymal and intraventricular hemorrhage: a study of infants with birth weights less than 1,500 gm. The Journal of pediatrics. 1978 Apr 1; 92(4):529–34. https://doi.org/10.1016/s0022-3476(78)80282-0 PMID: 305471
22. Easa D, Tran A, Bingham W. Noninvasive intracranial pressure measurement in the newborn: an alternate method. American Journal of Diseases of Children. 1983 Apr 1; 137(4):332–5. https://doi.org/10.1001/archpedi.1983.02140300014004 PMID: 6829512
23. Guihard-Costa AM, Larroche JC. Differential growth between the fetal brain and its infratentorial part. Early human development. 1990 Jun 1; 23(1):27–40. https://doi.org/10.1016/0378-3782(90)90126-4 PMID: 2209474
24. Hoffmann KH, Marx D, Botkin ND. Drag on spheres in micropolar fluids with non-zero boundary conditions for microrotations. Journal of Fluid Mechanics. 2007 Nov 10; 590:319–30.
25. Turova V, Botkin N, Alves-Pinto A, Blumenstein T, Rieger-Fackeldey E, Lampe R. Modeling autoregulation of cerebral blood flow using viability approach. InInternational Symposium on Dynamic Games and Applications 2016 Jul 12 (pp. 345–363). Birkhäuser, Cham.
26. Erdoğan ME. Polar effects in the apparent viscosity of a suspension. Rheologica Acta. 1970 Sep 1; 9(3):434–8.
27. Papautsky I, Brazzle J, Ameel T, Frazier AB. Laminar fluid behavior in microchannels using micropolar fluid theory. Sensors and actuators A: Physical. 1999 Mar 9; 73(1–2):101–8.
28. Linderkamp O, Stadler AA, Zilow EP. Blood viscosity and optimal hematocrit in preterm and full-term neonates in 50–to 500–μm tubes. Pediatric research. 1992 Jul; 32(1):97–102. https://doi.org/10.1203/00006450-199207000-00019 PMID: 1635852
29. Peyrounette M, Davit Y, Quintard M, Lorthois S. Multiscale modelling of blood flow in cerebral microcirculation: Details at capillary scale control accuracy at the level of the cortex. PloS one. 2018 Jan 11; 13(1):e0189474. https://doi.org/10.1371/journal.pone.0189474 PMID: 29324784
30. Vidotto E, Koch T, Köppl T, Helmig R, Wohlmuth B. Hybrid models for simulating blood flow in microvascular networks. Multiscale Modeling & Simulation. 2019; 17(3):1076–102.
31. Desjardins CL, Duling BR. Microvessel hematocrit: measurement and implications for capillary oxygen transport. American Journal of Physiology-Heart and Circulatory Physiology. 1987 Mar 1; 252(3):H494–503. https://doi.org/10.1152/ajpheart.1987.252.3.H494 PMID: 3548438
32. Pries AR, Neuhaus D, Gaehtgens P. Blood viscosity in tube flow: dependence on diameter and hematocrit. American Journal of Physiology-Heart and Circulatory Physiology. 1992 Dec 1; 263(6):H1770–8. https://doi.org/10.1152/ajpheart.1992.263.6.H1770 PMID: 1481902

33. Tomiyama Y, Brian JE Jr, Todd MM. Plasma viscosity and cerebral blood flow. American Journal of Physiology-Heart and Circulatory Physiology. 2000 Oct 1; 279(4):H1949–54. https://doi.org/10.1152/ajpheart.2000.279.4.H1949 PMID: 11009484

34. Rebel A, Ulatowski JA, Kwansa H, Bucci E, Koehler RC. Cerebrovascular response to decreased hematocrit: effect of cell-free hemoglobin, plasma viscosity, and CO2. American Journal of Physiology-Heart and Circulatory Physiology. 2003 Oct; 285(4):H1600–8. https://doi.org/10.1152/ajpheart.00077.2003 PMID: 12816746

35. Tao R, Huang K. Reducing blood viscosity with magnetic fields. Physical Review E. 2011 Jul 12; 84(1):011905. https://doi.org/10.1103/PhysRevE.84.011905 PMID: 21867211

36. Payne S. Cerebral autoregulation: control of blood flow in the brain. Cham: Springer International Publishing; 2016 Jun 24.

37. Zauner A, Muizelaar JP. Brain metabolism and cerebral blood flow. Head injury. 1997:89–99.

38. Younkin DP, Reivich M, Jaggi JL, Obrist WD, Delivoria-Papadopoulos M. The effect of hematocrit and systolic blood pressure on cerebral blood flow in newborn infants. Journal of Cerebral Blood Flow & Metabolism. 1987 Jun; 7(3):295–9. https://doi.org/10.1038/jcbfm.1987.66 PMID: 3584264

39. Linder N, Haskin O, Levit O, Klinger G, Prince T, Naor N, et al. Risk factors for intraventricular hemorrhage in very low birth weight premature infants: a retrospective case-control study. Pediatrics. 2003 May 1; 111(5):e590–5. https://doi.org/10.1542/peds.111.5.e590 PMID: 12728115

40. Dekom S, Vachhani A, Patel K, Barton L, Ramanathan R, Noori S. Initial hematocrit values after birth and peri/intraventricular hemorrhage in extremely low birth weight infants. Journal of Perinatology. 2018 Nov; 38(11):1471–5. https://doi.org/10.1038/s41372-018-0224-6 PMID: 30206347

41. Sola MC, del Vecchio A, Edwards TJ, Suttner D, Hutson AD, Christensen RD. The relationship between hematocrit and bleeding time in very low birth weight infants during the first week of life. Journal of Perinatology. 2001 Sep; 21(6):368–71. https://doi.org/10.1038/sj.jp.7210546 PMID: 11593370

42. Hambleton G, Wigglesworth JS. Origin of intraventricular haemorrhage in the preterm infant. Archives of Disease in Childhood. 1976 Sep 1; 51(9):651–9. https://doi.org/10.1136/adc.51.9.651 PMID: 999324

43. Parodi A, Govaert P, Horsch S, Bravo MC, Ramenghi LA. Cranial ultrasound findings in preterm germinal matrix haemorrhage, sequelae and outcome. Pediatric research. 2020 Mar; 87(1):13–24. https://doi.org/10.1038/s41390-019-0636-9 PMID: 31652434